Semisynthetic latrunculin B analogs: Studies of actin docking support a proposed mechanism for latrunculin bioactivity

Sucheta Kudrimoti [a], Safwat A. Ahmed [f], Pankaj R. Daga [d], Amir E. Wahba [a], Sherief I. Khalifa [g], Robert J. Doerksen [d,e], Mark T. Hamann [a,b,c,e,*]

[a] Department of Pharmacognosy, The University of Mississippi, University, MS 38677-1848, United States
[b] Department of Pharmacology, The University of Mississippi, University, MS 38677-1848, United States
[c] Department of Chemistry and Biochemistry, The University of Mississippi, University, MS 38677-1848, United States
[d] Department of Medicinal Chemistry, The University of Mississippi, University, MS 38677-1848, United States
[e] The National Center for Natural Products Research, The University of Mississippi, University, MS 38677-1848, United States
[f] Department of Pharmacognosy, Faculty of Pharmacy, Suez Canal University, Ismailia, Egypt
[g] Department of Pharmacy Practice and Clinical Pharmacy, Faculty of Pharmacy, Msir International University, Cairo, Egypt

ARTICLE INFO

ABSTRACT

Latrunculins are unique macrolides containing a thiazolidinone moiety. Latrunculins A, B and T and 16-epi-latrunculin B were isolated from the Red Sea sponge *Negombata magnifica*. N-Alkylated, O-methylated analogs of latrunculin B were synthesized and biological evaluation was performed for antifungal and antiprotozoal activity. The natural latrunculins showed significant bioactivity, while the semisynthetic analogs did not. Docking studies of these analogs into the X-ray crystal structure of G-actin showed that, in comparison with latrunculins A and B, N-alkylated latrunculins did not dock satisfactorily. This suggests that the analogs do not fit well into the active site of G-actin due to steric clashes and provides an explanation for the absence of bioactivity.

Published by Elsevier Ltd.

1. Introduction

Latrunculins are architecturally unique marine metabolites which were first isolated from the Red Sea sponge *Negombata magnifica* (formerly *Latruncilin magnifica*).[1] Coral reefs of the Red Sea are densely populated with colonies of the *N. magnifica* sponge, which are apparently free from predation due to chemical defense.[2] Squeezing this sponge leads to a secretion of a reddish fluid which has been shown to cause poisoning in fish. A detailed study of this excretion by Kashman's group led to the discovery of latrunculins, which are 14- and 16-membered lactones and the first natural products known to contain a 2-thiazolidinone moiety, **1–4** (Fig. 1).[2,3] These macrolides were also later found in taxonomically unrelated organisms from different geographic locations, signifying that the actual producer or origin of these curious secondary metabolites could be symbiotic microbes.[4]

Over the past years macrolides of marine source have continued to be of interest due to their varied biological activities. In addition to the significant ichthyotoxic properties, the latrunculins are also cytotoxic to tumor cells and antiviral.[5] The significant physiological properties of latrunculins has led to their extensive utilization as biochemical tools. Latrunculins alter cell shape and inhibit the microfilament mediated processes of meiosis, fertilization, early development, force development in muscles, and even influence protein kinase C signaling.[6] These metabolites play an important interfering role in actin polymerization[7] and cytoskeletal coordination which are essential in cell locomotion and many forms of motility, including phagocytosis and cytokinesis. Actin-binding proteins control the contractile machinery of smooth muscle cells and play a significant role in controlling the structural framework that surrounds and supports the contractile apparatus. Actin-binding proteins regulate the dynamic equilibrium that exists between actin monomers (G-actin) and actin polymers or filaments (F-actin). A recent report shows that aging skin appears to look younger when treated with this type of metabolite.[8] It was shown that the increasing volume of filamentous F-actin fibers is a major source of the stiffness of human epithelial cells and repairing the elasticity in skin cells can be achieved by chemically halting F-actin polymerization. The treatments evaluated contained compounds known to intervene with F-actin polymerization such as cytochalasin B, cytochalasin D, and latrunculins A and B. These studies furnish insight and potential for both biological and pharmaceutical applications for these natural products. Skin treated with cytochalasin B progressively became softer with fewer wrinkles.[8] Recent progress in the study of actin interaction with small marine molecules
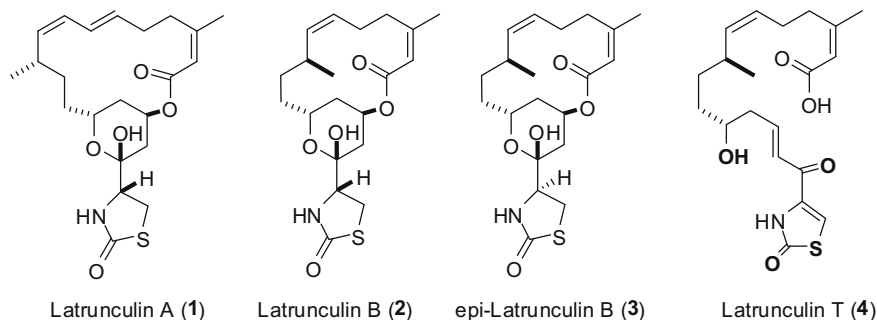
Figure 1. Latrunculin macrolides.

prompted our design and synthesis of modified analogs. Previous studies have focused on the synthesis of analogs with an aromatic and sulfonyl functional group attached at the hydroxy group. The majority of these analogs were surprisingly inactive against various cancer cell lines as well as bacteria and protozoa. These data have shown that the pyran ring hydroxy group is clearly essential for cytotoxicity and actin binding.[9]

In this study, we report the synthesis and biological evaluation of a small series of N-alkyl, O-methyl derivatives of latrunculin B having a varying-length carbon chain substituted at the nitrogen of the thaizolidinone moiety. Since previous studies have shown the importance of a free hydroxy group for the biological activity, we also carried out hydrolysis of the protected hydroxy group of the N-decyl, O-methyl derivative to check if protection of this OH in the molecules was responsible for the weaker activity. We used computational docking studies to study the predicted binding mode of the newly synthesized analogs to G-actin.

2. Results and discussion

2.1. Natural latrunculins isolation

Analysis of the crude extract of *N. magnifica* by TLC indicated the presence of latrunculin B and other related metabolites. Flash column chromatography (normal-phase) of the methanol/dichloromethane extract provided several fractions. After several extensive chromatographic steps, **2** was afforded as the major metabolite as well as **1**, **3**, and **4** as minor metabolites. Compounds **1**–**4** were identified by comparison of their spectroscopic properties to those in the literature.[2a,10,11]

2.2. Synthesis of N-alkylated analogs

Synthetic derivatives were prepared using latrunculin B (**2**) as a starting material. Latrunculins are known to be highly sensitive to both acidic and basic conditions.[12] This instability can be consider-

ably reduced through the acetalization of the lactol functionality by protection of the hydroxy group of the tetrahydropyran (THP) ring. This protection was accomplished through the treatment of **2** with methanol in the presence of a catalytic amount of boron-tri-fluoro-etherate to yield **5** (Scheme 1). N-Alkylation of thiazolidine ring was then carried out on the amidic nitrogen of **5** by using sodium hydride in the presence different alkyl halides in tetrahydrofuran (THF) under nitrogen atmosphere (Scheme 1). The N-alkylated products (**6**–**11**) were confirmed by ^{1}H NMR data in which N-alkylation was confirmed by the absence of an N–H peak at 5.90 ppm. N-Decyllatrunculin B (**12**) was obtained by the catalytic acid hydrolysis of the acetal functionality in **11**.

2.3. Biological testing

The isolated compounds **1**–**4**, O-methylated latrunculin B (**5**) (Table 1), and N-alkylated derivatives (**6**–**12**) were evaluated for anti-fungal and anti-protozoal activity (*Saccharomyces cerevisiae* NRRL Y-2034, *Aspergillus flavus* NRRL 501, and *Candida albicans*) using the twofold dilution method.[13] Latrunculin T (**4**) was found to be more active than other isolated latrunculins against *S. cerevisiae* NRRL Y-2034 (MIC = 32 μg/M). Latrunculin A (**1**) was found to be active against *C. albicans* (MIC = 60 μg/M), and *A. flavus* NRRL 501 (MIC = 60 μg/M). The alkylated latrunculin B derivatives **5**–**12** were evaluated for antimalarial and antimicrobial activity but were found to be inactive.
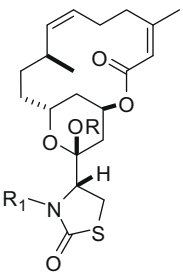
2.4. Actin docking studies

2.4.1. Actin X-ray structure

To check the effect of the substitutions on G-actin docking and by implication on actin binding, stepwise docking studies were carried out. Docking of latrunculins A and B has been reported recently by Fürstner et al.[14] using AUTODOCK followed by optimization. Fürstner et al. used 1ESV,[15] a complex of actin with latrunculin A (2.00 Å resolution), for their docking studies. How-
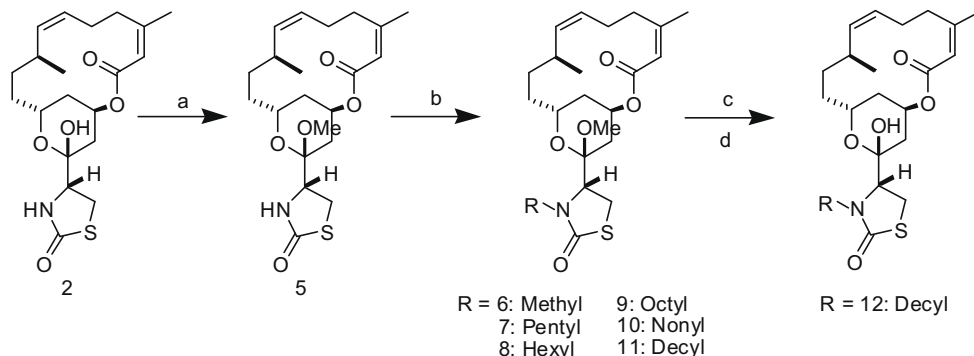
Scheme 1. Synthesis of the N-alkyl derivatives of latrunculin B. Reagents and conditions: (a) BF₃·OEt₂, MeOH, rt; (b) NaH, THF, R–X, 0 °C, rt; (c) concd H₂SO₄ (10 μL), THF, rt; (d) H₂O.

Table 1
GOLD docking scores for the latrunculin B analogs

Analog	R	R_1	GOLD Score
2	H	H	70.2
5	Me	H	48.0
6	Me	Methyl	21.7
7	Me	Pentyl	18.1
8	Me	Hexyl	21.1
9	Me	Octyl	23.1
10	Me	Nonyl	28.5
11	Me	Decyl	32.1
12	H	Decyl	35.5

ever, one of the active site amino acids showing hydrogen bonding interaction with the ligand, Glu207, is not resolved in 1ESV. Hence, docking into that crystal structure is unreliable. We instead used an alternative co-crystal structure of latrunculin A in actin, 1RDW (2.30 Å),[16] in our work.

2.4.2. Latrunculins A (1) and B (2)

As part of our research on latrunculins reported recently,[17] GOLD[18] was able to dock **1** into the G-actin ATP binding site in a manner similar to that of the actin-latrunculin A co-crystal structures. Merging of the docked pose with the protein structure extracted from the crystal structure and minimization of the complex resulted in the same hydrogen bonding and van der Waals interactions as those in the crystal structure. Compound **2**, using the same procedure for docking and minimization, yielded a very similar pose to that of **1**. All the hydrogen bonding interactions observed in the X-ray co-crystal structure of **1** in actin were reproduced for **1** and for **2** as well (Fig. 2). The overlay of the two

latrunculins with the crystal structure is shown in Figure 3. The docking scores (Table 1) were 90.7 (**1**) and 70.0 (**2**) for the two molecules. The binding energies calculated were −84.8 and −74.5 kcal/mol for **1** and **2**, respectively.

2.4.3. O-Methylated latrunculin B (5)

In this work, latrunculin B was then modified by replacing the hydroxy group on the pyran ring with methoxy to obtain O-methylated latrunculin B (**5**). The docking pose obtained for **5** was reasonably similar to that of **1** and **2**. The docking score for this analog was 48.0 while that of **2** was 70.2. The ligand was then merged into the active site and minimization was carried out. The binding energy was calculated to be −53.1 kcal/mol, so it is predicted not to bind as well as **2**. The final minimized binding pose of **5** is shown in Figure 4. Minimization of the complex resulted in the side chain of the Glu207 residue moving by ≈0.71 Å and that of Tyr69 moving by ≈1.2 Å away from their original position in the crystal structure. Hence we predict that the O-methylated analog will best bind to
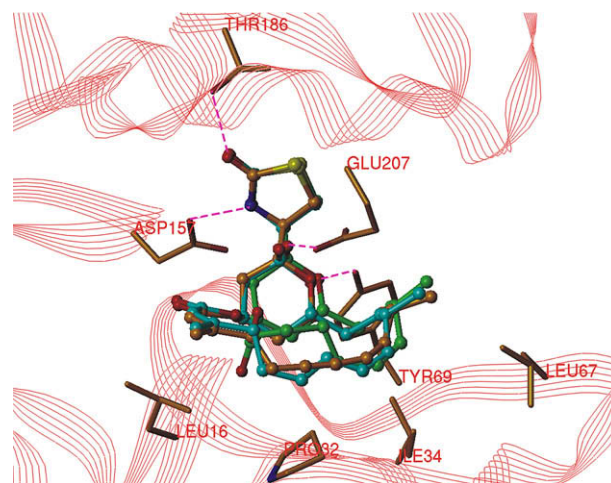

Figure 3. Optimized binding pose of latrunculin A (**1**) (ball-and-stick, C cyan) and latrunculin B (**2**) (ball-and-stick, C green) in actin (red ribbon mode), shown overlapped with **1** from 1RDW (ball-and-stick, C gold); key H-bonds are shown (pink dashed lines).
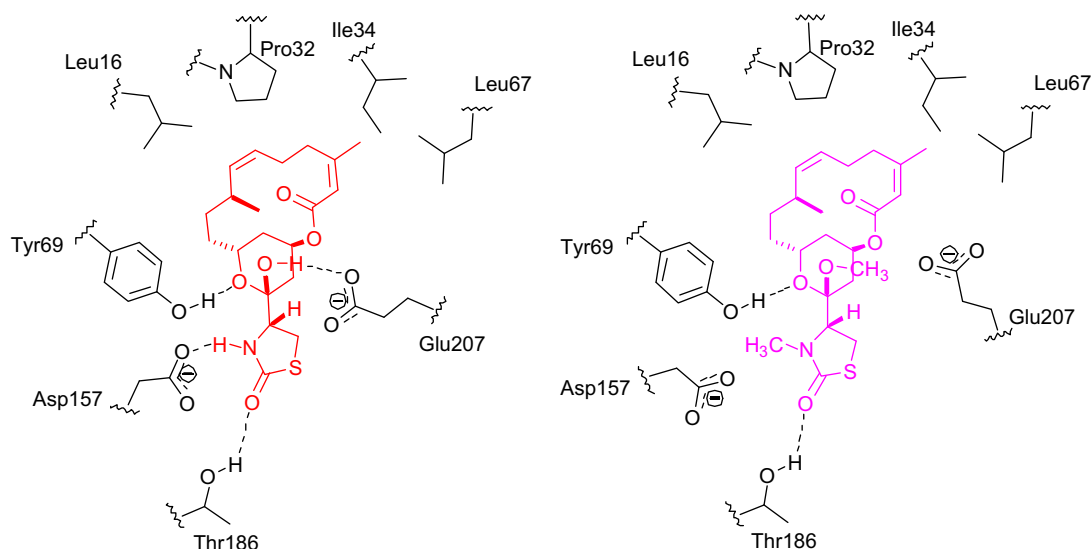

Figure 2. Schematic representation of the non-bonding interactions shown by latrunculin B (**2**) (left) and compound **6** (right) with actin.
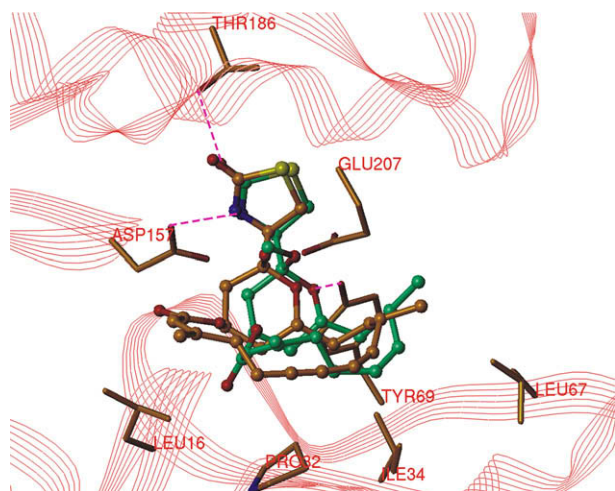
Figure 4. Optimized binding pose of O-methylated latrunculin B (**5**) (ball-and-stick, C bluegreen) in actin (red ribbon mode), shown overlapped with optimized latrunculin A (**1**) (ball-and-stick, C gold, from 1RDW.pdb); key H-bonds are shown (pink dashed lines). Glu207 and Tyr69 residues have moved away from the binding site compared to the crystal structure.

the actin active site if there is some movement of active site residue side chains. The methyl substitution pushed the ligand slightly away from the location of **2** in its docked pose. All the hydrogen bonding interactions observed in the X-ray co-crystal structure of **1** in actin were also seen for **5** except for that with Glu207, which is to the pyran ring hydroxyl in **1**.

2.4.4. N-Alkylated latrunculins

Each of the semi-synthetic latrunculins (**6–12**) were docked into the active site using the same procedure. GOLD produced 10 different conformations for each molecule. Depending upon the position of the five-membered thiazolidinone ring and macrocyclic lactone ring, all the docked conformations collectively could be divided into three different clusters. Representatives of the three different docking poses are shown in Figure 5. In all clusters, the thiazolidinone ring moved away from the binding pocket it occupies for **1** or **2**, and in the pose shown in Figure 5a the pyran ring also was greatly displaced. One of the docked conformations (shown in Fig. 5c) was closest to the crystal structure. However, only two of the hydrogen bonding interactions, observed for **1** bound into G-actin in 1RDW, were reproduced: the carbonyl oxygen was found to be H-bonded to Thr186 and the pyran ring O showed H-bonding interaction with Tyr69. Figure 2 illustrates that methylation of the amidic nitrogen and the hemiacetal functionality in **6** resulted in loss of two hydrogen bonding interactions, with

Asp157 and Glu207, respectively, while the hydrogen bonding interactions with Tyr69 and Thr186 and hydrophobic interactions with Leu16, Pro32, Ile34, and Leu67 found for **2** were maintained for **6**. The macrocyclic ring was found to be shifted also. In the two other cases (Fig. 5a and b), it was obvious that GOLD was not able to dock these molecules into the active site of G-actin. The docking scores for the N-alkylated latrunculins are shown in Table 1. In comparison with latrunculins A and B, **6–12** showed very low scores between 18 and 36, suggesting that these molecules have extremely low binding affinity toward G-actin. The docking poses show that they would not be able to fit well into the active site of G-actin due to steric clashes. There is a slight increase in docking score with increase in alkyl chain length but this can be attributed to the increase in van der Waals binding of the alkyl sidechain with hydrophobic groups away from the thiazolidinone binding pocket and in fact the longer side chains make it harder for the N-alkylated latrunculins to fit into the actin binding pocket.

3. Conclusions

We have synthesized O-methylated-N-alkylated-latrunculin B analogues and evaluated their cytotoxicity and antimicrobial activity. The docking studies demonstrated why free NH and OH groups of latrunculin B (**2**) are essential to have any activity for the above synthesized compounds. The O-methylated **5** had reduced binding to G-actin since it had one fewer hydrogen bond. The O-methylated-N-alkylated analogues could not fit into the G-actin latrunculin binding pocket.

4. Experimental

4.1. General experimental procedures

The ^{1}H and ^{13}C NMR spectra were recorded in CDCl$_3$ on a Bruker DRX NMR spectrometer operating at 400 MHz for ^{1}H and 75 MHz for ^{13}C. Chemical shift (δ) values are expressed in parts per million (ppm) and are referenced to the residual solvent signals of CDCl$_3$. Optical rotations were measured with a JASCO DIP-310 digital polarimeter. The high resolution ESI-MS spectra were measured using a Bruker Daltonic (GmbH, Germany) micro-TOF series with electrospray ionization.

4.2. Isolation and characterization

The specimen of the sponge N. magnifica utilized for this study was collected by SCUBA at a depth of 15 m off Hurghada in the Egyptian Red Sea. The sponge material was frozen immediately
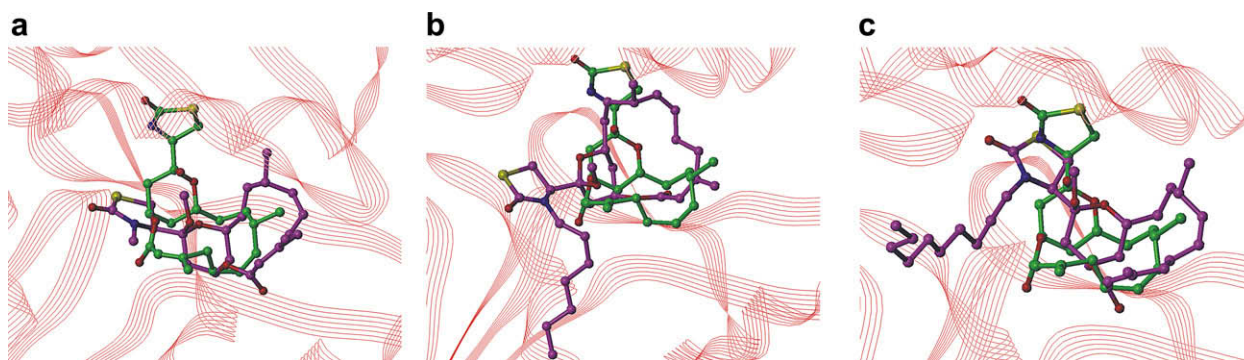

Figure 5. Three different binding pose clusters predicted by GOLD for N-alkylated latrunculin B analogs (represented by (a) **6**; (b) **10**; and (c)) **11**. The images portray that these analogs do not bind to the active site in a similar pose to those of **1** (X-ray structure shown, C green) and **2**. One of the docked conformations, (c), was the closest to the pose of **1** in the crystal structure, though even in that case not all the hydrogen bonding interactions observed in 1RDW were reproduced.

and kept frozen at −20 °C until processed. The voucher specimen is deposited at the Zoological Museum of the University of Amsterdam, under the registration no. ZMAPOR 18968. The sponge occurs as branching, red colored colonies at a depth of 6.0–15.0 m. Colonies of these sponges grow attached to exposed rocks or descending rocky slopes. Single branches usually measure 30–40 cm long and 1.5–2.0 cm thick. The sponges (in the dried state) are erect and composed of short, curved, flanged, narrow fans of different lengths with a restricted base of attachment. Surface textures of dry sponges are fibrous and roughened. The specimen of sponge viewed microscopically revealed that megascleres are arranged uniformly within fibers and clearly differentiated into primary and secondary tracts. The sponge material was identified and confirmed by Professor Rob W. M. VanSoest, Faculty of Science, Zoological Museum, Amsterdam. The sponge sample was freeze-dried (1 kg dry weight), ground and extracted with a mixture of $MeOH/CH_2Cl_2$ (1:1) (3 × 2 L) at room temperature. The extract was evaporated under vacuum to give 250 g of red oil. This extract was subjected to vacuum liquid chromatography on flash silica using hexane, ethyl acetate, and methanol gradient. Fractions eluted from 30% to 60% ethyl acetate in hexane were combined and concentrated to afford 60 g of material. Purification of this fraction was carried out by flash column chromatography on silica gel using hexane/ethyl acetate (85:15). Relatively non-polar fractions were combined. Final purification was carried out on RP-C18-HPLC using a mobile phase consisting of acetonitrile and water (60:40 v/v) to afford **1** (5 mg), **2** (4 g), and **3** (2 mg).

The polar fractions were combined and rechromatographed by flash column chromatography on silica gel using 2% methanol in chloroform. Final purification was carried out on sephadex LH-20 using methanol/chloroform (1:1) to afford **4** (14 mg).

4.3. Acetalization of 2

To a solution of **2** (0.395 g, 0.001 mmol) in MeOH, a catalytic amount of Et_2O–BF_3 was added. The mixture was stirred overnight and was neutralized with 10% aq. $NaHCO_3$ solution. The crude product was extracted with DCM (3 × 30 mL) and the organic layer was dried over anhydrous Na_2SO_4 then evaporated under reduced pressure. The residue was purified by silica column (9:1 hexane/acetone).

4.3.1. 15-MethoxyLat B (5)

(0.327 g, 80%); $[\alpha]_D^{25}$ 23.9 (*c* 0.11, MeOH); ^{1}H NMR (CDCl$_3$) δ (ppm): 5.9 (s, NH), 5.70 (s, 2-H), 5.17 (br s, 13-H), 5.25 (td, *J* = 11.4, 3.3, 6-H), 5.05 (td, *J* = 11.4, 1.6, 7-H), 4.2 (br t, *J* = 11.4, 11-H), 3.80 (dd, *J* = 12.0, 2.2, 16H), 3.40 (dd, *J* = 12.0, 2.2, 17-H), 3.29 (s, OCH$_3$), 2.75–1.0 (m, 5,5′, 4,4′, 9,9″, 10,10′, 12,12′, 14,14′-H), 1.90 (s, 20-CH$_3$), 0.90 (s, 19-CH$_3$). HRMS *m/z* calcd for $C_{21}H_{32}NO_5S$ (M+H$^+$) 410.2001, found 410.1997.

4.4. Alkylation of nitrogen of the thiazolidinone

To a suspension of sodium hydride (0.062 mmol) in dry THF, was slowly added methoxy Lat-B (0.045 mmol) at 0 °C. The mixture was stirred for one hour, then alkyl halide (2.4 mmol) was added and the reaction mixture stirred for 6–8 h under nitrogen atmosphere. Ether and water were added and the organic layer was dried over anhydrous Na_2SO_4. The residue was purified by column chromatography to yield pure *N*-alkyl derivative of Lat-B.

4.4.1. 15-Methoxy-*N*-methyl-Lat B (6)

(10 mg, 53%); $[\alpha]_D^{25}$ 27.2 (*c* 0.11, MeOH); ^{1}H NMR (CDCl$_3$) δ (ppm): 5.70 (s, 2-H), 5.17 (br s, 13-H), 5.25 (td, *J* = 11.4, 3.3, 6-H), 5.05 (td, *J* = 11.4, 1.6, 7-H), 4.24 (br t, *J* = 11.4, 11-H), 3.80 (dd, *J* = 12.0, 2.2, 16-H), 3.40 (dd, *J* = 12.0, 2.2, 17-H), 3.29 (s, OCH$_3$),

3.20 (s, N-CH$_3$), 2.75–1.00 (m, 5,5′, 4,4′, 9,9′, 10,10′, 12,2′, 14,14′-H), 1.90 (s, 20-CH$_3$), 0.90 (s, 19-CH$_3$). HRMS *m/z* calcd for $C_{22}H_{33}NO_5SNa$ (M+Na$^+$) 446.1977, found 446.1981.

4.4.2. 15-Methoxy-*N*-pentyl-Lat B (7)

(11 mg, 52%); $[\alpha]_D^{25}$ 22.1 (*c* 0.11, MeOH); ^{1}H NMR (CDCl$_3$) δ (ppm) 5.70 (s, 2-H), 5.17 (br s, 13-H), 5.25 (td, *J* = 11.4, 3.3, 6-H), 5.05 (td, *J* = 11.4, 1.6, 7-H), 4.24 (br t, *J* = 11.4, 11-H), 3.80 (dd, *J* = 12.0, 2.2, 16-H), 3.40 (dd, *J* = 12.0, 2.2, 17-H), 3.29 (s, OCH$_3$), 3.15 (t, N-CH$_2$), 2.75–1.0 (m, 5,5′, 4,4′, 9,9′, 10,10′, 12,12′, 14,14′-H, CH$_3$ and (CH$_2$)$_3$), 1.91 (s, 20-CH$_3$), 0.92 (s, 19-CH$_3$). HRMS *m/z* calcd for $C_{26}H_{41}NO_5SNa$ (M+Na$^+$) 502.2603, found 502.2611.

4.4.3. 15-Methoxy-*N*-hexyl-Lat B (8)

(11 mg, 51%); $[\alpha]_D^{25}$ 27.5 (*c* 0.11, MeOH); ^{1}H NMR (CDCl$_3$) δ (ppm) 5.70 (s, 2-H), 5.17 (br s, 13-H), 5.25 (td, *J* = 11.4, 3.3, 6-H), 5.05 (td, *J* = 11.4, 1.6, 7-H), 4.24 (br t, *J* = 11.4, 11-H), 3.80 (dd, *J* = 12.0, 2.2, 16-H), 3.40 (dd, *J* = 12.0, 2.2, 17-H), 3.29 (s, OCH$_3$), 3.19 (s, N-CH$_2$), 2.75–1.00 (m, 5,5′, 4,4′, 9,9′, 10,10′, 12,12′, 4,14′-H, CH$_3$ and (CH$_2$)$_4$), 1.90 (s, 20-CH$_3$), 0.90 (s, 19-CH$_3$). HRMS *m/z* calcd for $C_{27}H_{43}NO_5SNa$ (M+Na$^+$) 516.2760, found 516.2769.

4.4.4. 15-Methoxy-*N*-octyl-LatB (9)

(12 mg, 52%); $[\alpha]_D^{25}$ 29.8 (*c* 0.11, MeOH); ^{1}H NMR (CDCl$_3$) δ (ppm) 5.70 (s, 2-H), 5.17 (br s, 13-H), 5.25 (td, *J* = 11.4, 3.3, 6-H), 5.05 (td, *J* = 11.4, 1.6, 7-H), 4.24 (br t, *J* = 11.4, 11-H), 3.80 (dd, *J* = 12.0, 2.2, 16-H), 3.40 (dd, *J* = 12.0, 2.2, 17-H), 3.29 (s,OCH$_3$), 3.21 (t, N-CH$_2$), 2.75–1.00 (m, 5,5′, 4,4′, 9,9′, 10,10′, 12,12′, 14,14′-H, CH$_3$ and (CH$_2$)$_6$), 1.90 (s, 20-CH$_3$), 0.90 (s, 19-CH$_3$). HRMS *m/z* calcd for $C_{29}H_{47}NO_5SNa$ (M+Na$^+$) 544.3072, found 544.3083.

4.4.5. 15-Methoxy-*N*-nonyl-Lat B (10)

(13 mg, 55%); $[\alpha]_D^{25}$ 27.2 (*c* 0.11, MeOH); ^{1}H NMR (CDCl$_3$) δ (ppm) 5.70 (s, 2-H), 5.17 (br s, 13-H), 5.25 (td, *J* = 11.4, 3.3, 6-H), 5.05 (td, *J* = 11.4, 1.6, 7-H), 4.24 (br t, *J* = 11.4, 11-H), 3.80 (dd, *J* = 12.0, 2.2, 16-H), 3.40 (dd, *J* = 12.0, 2.2, 17-H), 3.29 (s, OCH$_3$), 3.21 (t, N-CH$_2$), 2.75–1.00 (m, 5,5′, 4,4′, 9,9′, 10,10′, 12,12′, 14,14′-H, CH$_3$ and (CH$_2$)$_7$), 1.90 (s, 20-CH$_3$), 0.90 (s, 19-CH$_3$). HRMS *m/z* calcd for $C_{30}H_{49}NO_5SNa$ (M+Na$^+$) 558.3229, found 558.3234.

4.4.6. 15-Methoxy-*N*-decyl-Lat B (11)

(12 mg, 50%); $[\alpha]_D^{25}$ 31.1 (*c* 0.11, MeOH); ^{1}H NMR (CDCl$_3$) δ (ppm) 5.70 (s, 2-H), 5.17 (br s, 13-H), 5.25 (td, *J* = 11.4, 3.3, 6-H), 5.05 (td, *J* = 11.4, 1.6, 7-H), 4.2 (br t, *J* = 11.4, 11-H), 3.80 (dd, *J* = 12.0, 2.2, 16-H), 3.40 (dd, *J* = 12.0, 2.2, 17-H), 3.29 (s, OCH$_3$), 3.21 (t, N-CH$_2$), 2.75–1.00 (m, 5,5′, 4,4′, 9,9′, 10,10, 12,12′, 14,14′-H, CH$_3$ and (CH$_2$)$_8$), 1.90 (s, 20-CH$_3$), 0.90 (s, 19-CH$_3$). HRMS *m/z* calcd for $C_{31}H_{51}NO_5SNa$ (M+Na$^+$) 572.3385, found 572.3377.

4.5. Hydrolysis of (11)

To a solution of **11** (0.062 mmol) in dry THF, H_2SO_4 (20 μmL) was added at room temperature. The mixture was stirred for one hour under nitrogen atmosphere, then poured into H_2O (10 mL). The crude product was extracted with ether (3 × 10 mL) and the organic layer was dried over anhydrous Na_2SO_4. The residue was purified by column chromatography to yield pure *N*-decyl derivative of Lat- B (**12**).

4.5.1. *N*-Decyl-Lat B (12)

(8 mg, 24%); $[\alpha]_D^{25}$ 19.1 (*c* 0.11, MeOH); ^{1}H NMR (CDCl$_3$) δ (ppm) 5.70 (s, 2-H), 5.17 (br s, 13-H), 5.25 (td, *J* = 11.4, 3.3, 6-H), 5.05 (td, *J* = 11.4, 1.6, 7-H), 4.2 (br t, *J* = 11.4, 11-H), 3.80 (dd, *J* = 12.0, 2.2, 16-H), 3.40 (dd, *J* = 12.0, 2.2, 17-H), 3.21 (t, N-CH$_2$), 2.75–1.00 (m, 5,5′, 4,4′, 9,9′, 10,10, 12,12′, 14,14′-H, CH$_3$ and (CH$_2$)$_8$), 1.90 (s, 20-CH$_3$),

0.90 (s, 19-CH$_3$). HRMS m/z calcd for $C_{30}H_{49}NO_5SNa$ (M+Na$^+$) 558.3229, found 558.3221.

5. Computational details

Hydrogen atoms were added to the protein crystal structure complex containing actin, ATP and latrunculin A and the resultant structure was used for the docking studies with GOLD 2.0.[18] For docking, the active site of the protein was defined as the pocket formed by atoms within a 10 Å sphere centered on the O of Glu207, which is involved in H-bonding to the ligand. For each docking run, GOLD's genetic algorithm was used to generate 100,000 solutions. The number of populations was set to 5. The selection pressure was 1.1. Two different scoring functions were used for the docking studies: GOLD Score and ChemScore. Both the scoring functions produced a similar docking conformation, so we reported only the GOLD Scores (higher score implies better binding). The docked conformation was merged into the binding cavity and the complex was then minimized in SYBYL 7.2[19] using the MMFF94 force field and charges, including only residues having any atom within an 8 Å sphere of Glu207 in the minimization (this included ATP). The binding energy (lower energy implies better binding) of ligands was calculated using the formula:

$$E_{binding} = E_{complex} - (E_{protein} + E_{ligand}).$$

Acknowledgments

Supplementary data

Supplementary data associated with this article can be found, in the online version, at doi:10.1016/j.bmc.2009.09.012.

References and notes

1. Neeman, I.; Fishelson, L.; Kashman, Y. *Mar. Biol.* **1975**, *30*, 293.
2. (a) Kashman, Y.; Groweiss, A.; Shmueli, U. *Tetrahedron Lett.* **1980**, *21*, 3629; (b) Gillor, O.; Carmeli, A.; Rahamim, Y.; Fishelson, Z.; Ilan, M. *Mar. Biotechnol.* **2000**, *2*, 213; (c) Hadas, E.; Shpigel, M.; Ilan, M. *Aquaculture* **2005**, *244*, 159; (d) Vilzny, B.; Amagata, T.; Mooberry, S. L.; Crew, P. *J. Nat. Prod.* **2004**, *67*, 1055.
3. Kashman, Y.; Groweiss, A.; Shmueli, U.; Lidor, R.; Blasberger, D.; Carmely, S. *Tetrahedron* **1985**, *41*, 1905.
4. Okuda, R. K.; Scheuer, P. J. *Experientia* **1985**, *41*, 1355.
5. (a) Spector, I.; Shochet, N. R.; Kashman, Y.; Groweiss, A. *Science* **1983**, *219*, 493; (b) Longley, R. E.; McConnell, O. J.; Essich, E.; Harmody, D. *J. Nat. Prod.* **1993**, *56*, 915; (c) Allingham, J. S.; Klenchin, V. A.; Rayment, I. *Cell. Mol. Life Sci.* **2006**, *18*, 1.
6. Coue, M.; Brenner, S. L.; Spector, I.; Korn, E. D. *FEBS Lett.* **1987**, *213*, 316.
7. Cimini, D.; Fioravanti, D.; Tanzarella, C.; Degrassi, F. *Chromosoma* **1998**, *107*, 479.
8. (a) Sokolov, I.; Iyer, S.; Woodworth, C. D. *Nanomedicine* **2006**, *2*, 31; (b) Sokolov, I. *Chem. Eng. News* **2006**, *84*, 34.
9. Wilkin, S. P. Ph.D. Thesis. *Isolation, Structure Elucidation and High-Throughput Lead Optimization Studies of Bioactive Secondary Metabolites from marine Invertebrates*; 2000 May.
10. Hoye, T. R.; Ayyad, S. N.; Eklov, B. M.; Hashish, N. E.; Shier, W. T.; El Sayed, K. A.; Hamann, M. T. *J. Am. Chem. Soc.* **2002**, *124*, 7405.
11. El Sayed, K. A.; Youssef, D. T.; Marchetti, D. J. *J. Nat. Prod.* **2006**, *69*, 219.
12. Blasberger, D.; Carmely, S.; Cojocaru, M.; Spector, I.; Shochet, N. R.; Kashman, Y. *Liebigs Ann. Chem.* **1989**, *12*, 1171.
13. Hansen, M. B.; Nielsen, S. E.; Berg, K. *J. Immunol. Methods* **1989**, *119*, 203.
14. Fürstner, A.; Kirk, D.; Fenster, M. D. B.; A, C.; De Souza, D.; Nevado, C.; Tuttle, T.; Thiel, W.; Müller, O. *Chem. Eur. J.* **2007**, *13*, 135.
15. Morton, W. M.; Ayscough, K. R.; McLaughlin, P. J. *Nature Cell Biol.* **2000**, *2*, 376–378.
16. Reutzel, R.; Yoshioka, C.; Govindasamy, L.; Yarmola, E. G.; Agbandje-McKenna, M.; Bubb, M. R.; McKenna, R. *J. Struct. Biol.* **2004**, *146*, 291.
17. Ahmed, S. A.; Odde, S.; Daga, P. R.; Bowling, J. J.; Mesbah, M. K.; Youssef, D. T.; Khalifa, S. I.; Doerksen, R. J.; Hamann, M. T. *Org. Lett.* **2007**, *9*, 4773.
18. Verdonk, M. L.; Cole, J. C.; Hartshorn, M. J.; Murray, C. W.; Taylor, R. D. *Proteins* **2003**, *52*, 609–623.
19. SYBYL 7.2, Tripos: 1699 South Hanley Rd., St. Louis, Missouri, 63144, USA.